Interspecies interactions in a model, mixed-species biofilm are determined by physiological traits and environmental factors

Running Title

Interspecies interactions in colony biofilms

Authors

Sean C. Booth[1†] and Scott A. Rice[1,2,3]

[1]The Singapore Centre for Environmental Life Sciences Engineering and [2]The School of Biological Sciences, Nanyang Technological University, Singapore

[3]The ithree Institute, The University of Technology Sydney, Australia

[†]Current address: Department of Zoology, University of Oxford, UK

Abstract

Interspecies interactions in bacterial biofilms have important impacts on the composition and function of communities in natural and engineered systems. To investigate these interactions, synthetic communities provide experimentally tractable systems. Colony biofilms are one such system that have been used for understanding the eco-evolutionary and biophysical forces that determine community composition and spatial distribution in biofilms. Prior work has focused on intraspecies interactions, using differently fluorescent tagged but identical or genetically modified strains of the same species. Here, we investigated how physiological differences determine the community composition and spatial distribution in synthetic biofilm communities of *Pseudomonas aeruginosa*, *Pseudomonas protegens* and *Klebsiella pneumoniae*. Visualizing this biofilm 'community morphology' microscopically revealed that the outcomes of interspecies interactions in multispecies biofilms are influenced by type IV pilus mediated motility, extracellular matrix secretion, environmental parameters and the specific species involved. These results indicate that the patterns observable in mixed species colony biofilms can be used to understand the mechanisms that drive interspecies interactions, which are dependent on the interplay between specific species' physiology and environmental conditions.

Introduction

Bacteria in natural and engineered systems interact with one another, which affects their ability to grow and survive under particular environmental conditions [1, 2]. Interactions between community members vary considerably; some interactions facilitate growth and survival, while others inhibit growth or even result in the death of one species [3]. Both faciliatory and inhibitory interactions can be mediated by secreted products, e.g. metabolite exchange [4] and antibiotic production [5] or by contact-dependent mechanisms, e.g. adhesion [6, 7] and Type VI secretion mediated killing [8]. Regardless of the specific mechanism of interaction, the composition and function of a community is influenced by the combination and sum of the various interactions between its constitutive members [9, 10].

Studies of the interactions between community members have shown how interspecies interactions influence community-intrinsic properties [11]. While competitive interactions between individual species are expected and common [12], often due to overlap of metabolic preferences [13], cooperative interactions can also be found in larger communities which enable increased biomass production [14] or resistance to antimicrobials [15]. Biofilms are ideal for examining the effect of interactions on a community, as cells are in close proximity to each other and are embedded within self-secreted biofilm matrix [16, 17]. For example, biofilms have been used to show how the genetic division of labor improves pellicle formation [18]. Using a synthetic, three-species community, we have shown that co-culture biofilms exhibit increased growth by particular members and enhanced stress tolerance for the entire community [19]. This occurred despite the community members competing for the same resources and was not observed for planktonic cultures, suggesting that spatial organization within biofilms is important for species interactions.

Colony biofilms, where bacteria are grown on a nutrient surface, are an efficient system for manipulating and visualizing the spatial distribution of different bacteria, but have mostly been used for studying eco-evolutionary dynamics [20]. Colony biofilms have been used to characterize various spatiotemporal aspects of microbial interactions including the co-localization of mutually auxotrophic strains of *Saccharomyces cerevisiae* [21, 22], the vertical separation of differently sized cells of *Escherichia coli* [23], the sequential range expansion of nitrate reducing *Pseudomonas stutzeri* [24], the spatial separation patterns of strains of *Vibrio cholerae* [25] or *Bacillus subtilis* [26] that differ in the quantity of extracellular matrix produced, and the proportion of different antibiotic resistant/sensitive strains of *P. aeruginosa* [27]. All of these studies have focused on different strains or mutants

of a single species (intraspecies interactions), differing only in the fluorescent marker they express and possibly in specifically altered genes. However, it is also clear that this approach has considerable potential to help unravel the mechanisms of interactions for mixed species biofilm communities.

In this study, we investigated the interactions between members of a model community consisting of *P. aeruginosa* PAO1, *P. protegens* Pf-5 (formerly *P. fluorescens* [28, 29]) and *K. pneumoniae* KP-1. These species can be commonly found in soils and habitats as varied as metalworking fluid or the gut of silk moths [30, 31]. When co-cultured in flow-cell biofilms, this community exhibits properties not observed in biofilms of the individual species including a relative increase in *K. pneumoniae*, sharing of resistance to sodium dodecyl sulfate allowing the sensitive species, *P. protegens*, to survive, [19] and reduced production of morphotypic variants for all species [32]. As colony biofilms offer some advantages compared to flow-cell biofilms, including higher throughput and the ability to image the entire biofilm, here we assessed interactions between each possible pair of these species by co-culturing them in a colony biofilm model. We determined whether these interactions were beneficial or detrimental by quantifying the area colonized by each species and qualifying where each species was found. By manipulating the community through using mutant strains and/or altered environmental conditions, we also show how organism-specific physiology determines interaction outcomes. This approach thus has the potential to identify gene systems and environmental conditions that underlie the interactions between bacterua. This work demonstrates that co-culturing in colony biofilms is a useful tool for determining the outcome of interactions between bacteria and visualizing the emergent properties of multi-species biofilms.

Materials and Methods

Strains, media and growth conditions: Colony biofilms were grown on minimal medium (48 mM Na_2HPO_4; 22 mM KH_2PO_4; 9 mM NaCl; 19 mM NH_4Cl; 2 mM $MgSO_4$; 0.1 mM $CaCl_2$; 0.04 mM $FeSO_4$; 2 mM glucose and 0.4% casamino acids) with either 1.5% or 0.6% agar in 24 well plates or 8 well Ibidi™ slides. Bacteria were inoculated into liquid medium from agar plates (because they are highly mucoid, wild-type *K. pneumoniae* strains were homogenized by passing repeatedly through a 30 G needle), the OD_{600} was standardized to 0.1 and 1/100 dilutions were used directly or mixed 1:1 or 1:1:1 and 0.5 µL was spotted at the center of each well. Spots were dried for 30 min in a laminar flow cabinet, plates were sealed with parafilm and incubated at room temperature. To confirm that mixtures were equal,

colony forming units (CFUs) were determined for the inoculum for each species/strain. If CFU counts indicated that the ratio of two mixed species/strains was more than 10 to 1 the sample was not used.

Table 1: Species and strains used in this study.

Species and strain	Genotypic and phenotypic characteristics	Fluorescent protein	Source or reference
P. aeruginosa PAO1	Wild-type	YFP, mCherry	ATCC BAA-47 [19], this study
P. aeruginosa PAO1 Small colony variant (SCV)	*pilT* Thr210 frameshift, twitching defect	YFP	[32]
P. protegens Pf-5	Wild-type	CFP, mCherry	ATCC BAA-477 [19], this study
K. pneumoniae KP-1	Wild-type	dsRed, CFP, YFP	[19]
K. pneumoniae KP-1 Non-mucoid variant (NMV)	UDP-glucose lipid carrier transferase Phe123Ile, matrix secretion defect	dsRed	[32]

For co-culture biofilms, only combinations of CFP or YFP labelled strains with dsRed or mCherry were used, with the exception of KP-1-YFP and Pf-5-CFP, due to issues of overlapping excitation and emission spectra. When multiple combinations were possible (e.g. KP-1-dsRed with KP-1-CFP or KP-1-YFP) both combinations were treated as equivalent i.e. the combination of dsRed with CFP was considered a replicate of combinations of dsRed with YFP.

Image acquisition: Colony biofilms were imaged on a Zeiss Axio Observer.Z1 inverted (24 well plates) or Imager.M2 upright (8 well slides) microscope using a HXP 120 C halogen

light source. On the Z1 a 5X/0.16 objective was used (total magnification 50x) and a 10X/0.3 objective on the M1 (100x total magnification). The filter sets (excitation/emission) used were: Zeiss Set 10 for CFP (450-490/515-565), Set 46 for YFP (490-510/520-550) and Set 31 (550-580/590-560) for dsRed and mCherry on the Z1. Set 43 (520-570/565-630) was used for dsRed and mCherry on the M1. Exposure times and focus were manually optimized for each sample then colonies were imaged using 'Tilescan' mode in Zeiss Zen (Blue edition) with 10% overlap. Twelve-bit images were captured using an AxioCamMRm3. Shading correction was applied using precaptured profiles of fluorescent slides.

Image Presentation: Representative images from each experimental combination were selected for presentation. Images were processed for viewing to improve contrast and remove artefacts, but only raw images were used for quantitative analysis. Images were corrected for flat-field illumination using BaSiC [33], stitched together in ImageJ [34, 35] and then the brightness was scaled manually for each channel in each image. In cases when there was high background signal, the background was either subtracted manually by selecting the colony area or by using the background subtraction tool.

Image Analysis: For full details, see the supplementary material. Tilescan images stitched together using Zeiss Zen were scaled down 1:10 to facilitate computational analyses, then processed using the R package 'imager' [36]. Each channel was normalized to a range of 0 to 1 and any background signal was subtracted. A mask of the colony biofilm was generated by taking the sum of all channels (including the inverted brightfield) then thresholding this image using the 'auto_thresh' function from the R package 'auto_thresholdr' [37], which was used to crop all channels for each image. This mask was also used to find the center of the colony and for conversion into polar coordinates. Radial/annular bins were generated by dividing the image angularly by 256 radians and every 100 µm outwards from the center. Within each of these bins, the mean was taken for each channel, then the ratio between channels was calculated by subtracting one from the other and dividing them by the sum of both ((c1-c2)/(c1+c2)). Thus, values can range from 1/-1 indicating only the presence of one strain, to 0, indicating an exactly equal mix of the two strains. The proportion of mixed bins was calculated by dividing the number of bins in the range -0.25:0.25 by the total number of bins. The individual channels of the processed images were separately thresholded using the 'imager::threshold()' function to determine the area occupied by each species. Manual inspection of images indicated that for *P. aeruginosa*, areas were slightly underestimated and for *K. pneumoniae*, areas were over estimated. Therefore, all images were also manually

quantified for comparison. For manual quantification, a combination of thresholding and area selection using the oval, wand or freehand selection was used. Comparison of manual and computational area quantification showed both methods produced similar results (Supplementary Figure 1).

Statistics: Analysis of variance, Tukey's honest significant difference post-hoc test and multiple-testing p-value adjustment were used to determine if there were significant differences in colony area between single and dual species biofilms. Separate analyses were calculated for the manual and computational area calculations, which agree and support the same conclusions (Supplementary Table 1), but the results from the manual quantification were considered more accurate so were used to draw conclusions about the data.

Results

Monospecies Biofilms

To compare patterns of interactions with previously published studies, we first examined intraspecies interactions by growing colony biofilms consisting of two strains of the same species (Figure 1). Qualitative inspection of the colonies after 24 and 48 h of growth indicated that each species differed in how they separate into sectors. *P. protegens* and *K. pneumoniae* showed clear segregation between their two differently coloured strains, although the shape of the borders differed. For *P. aeruginosa*, separation into sectors was only apparent at 48 h and the borders between strains were less distinct than for the other species. To better characterize the differences in colony growth, quantitative analyses were performed using multiple replicates by dividing images into radial/annular bins and calculating the ratio between the two strains in each bin. Based on this binning procedure, the percentage of mixed bins in each image was determined as a measure of how much the colony biofilm consisted of co-localized strains (Figure 1, G). Over 75% of the bins were mixed in the *P. aeruginosa* biofilms compared to 25% or less in the other two species. Even at the leading edge of *P. aeruginosa* biofilms that appeared to consist of a single strain, cells of both colours were present and were well mixed (Supplementary Video 1). The movement and mixing of the two strains was visible 500 µm inward from the colony edge (Supplementary Video 2). For all three species, there was no change in mixing between 24 and 48 h.

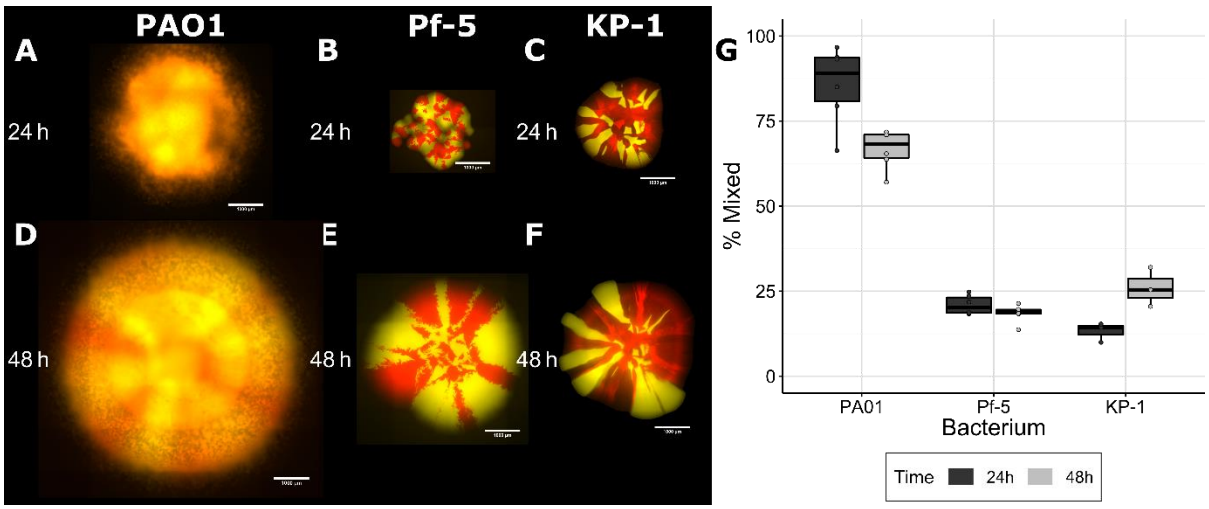

Figure 1: Colony biofilms consisting of *P. aeruginosa* PAO1 (A, D), *P. protegens* Pf-5 (B, E) or *K. pneumoniae* KP-1 (C, F). Each species was labeled separately with two different fluorescent protein genes and are presented here as red or yellow (false colouring). Strains were mixed 1:1 at the time of inoculation and colonies were imaged after 24 and 48 h of growth. Scale bars indicate 1000 µm. Overlap between differently labeled strains (G) was calculated from raw images ($n \geq 3$). Boxplots are presented in Tukey style.

Dual Species Biofilms

In contrast to monospecies biofilms, dual species colony biofilms differed in the area colonized and mixing of species (Figure 2). None of the combinations of species separated into clear sectors, as observed for the dual-strain biofilms described above, and instead formed different patterns. *P. aeruginosa* was only found around the perimeter of *P. protegens* colonies after 48 h and these species did not mix at either timepoint. While *P. aeruginosa* appeared to be restricted to the interior of the colony when cultured with *K. pneumoniae*, closer inspection of brightfield images (Supplementary Figure 2) showed that *P. aeruginosa* was also present around the outside perimeter of *K. pneumoniae*. This combination changed from unmixed (<25%) at 24 h to mixed at 48 h (~75%). When grown with *K. pneumoniae*, *P. protegens* grew around the outer edge of the colony and these species were also mixed (~75%) at 48 h. The amount of area covered by each strain in the dual-species biofilms was compared to the area covered by single species biofilms (Figure 2, H, Supplementary Table 1). At 24 h, the area covered by *P. aeruginosa* (~8 mm^2) was lower when co-cultured with *P. protegens* (~2 mm^2) and was similarly reduced at 48 h, from ~70 mm^2 (monospecies) compared to ~35 mm^2 (dual species). In contrast, there was no difference in the area covered by *P. protegens* when co-cultured with *P. aeruginosa*, although it was decreased at 24 h, but

not 48 h, with *K. pneumoniae*. The area covered by *K. pneumoniae* increased when co-cultured with *P. aeruginosa* from ~5 to ~10 mm^2 at 24 h and ~12 to ~40 mm^2 at 48 h, but was not affected by *P. protegens*.

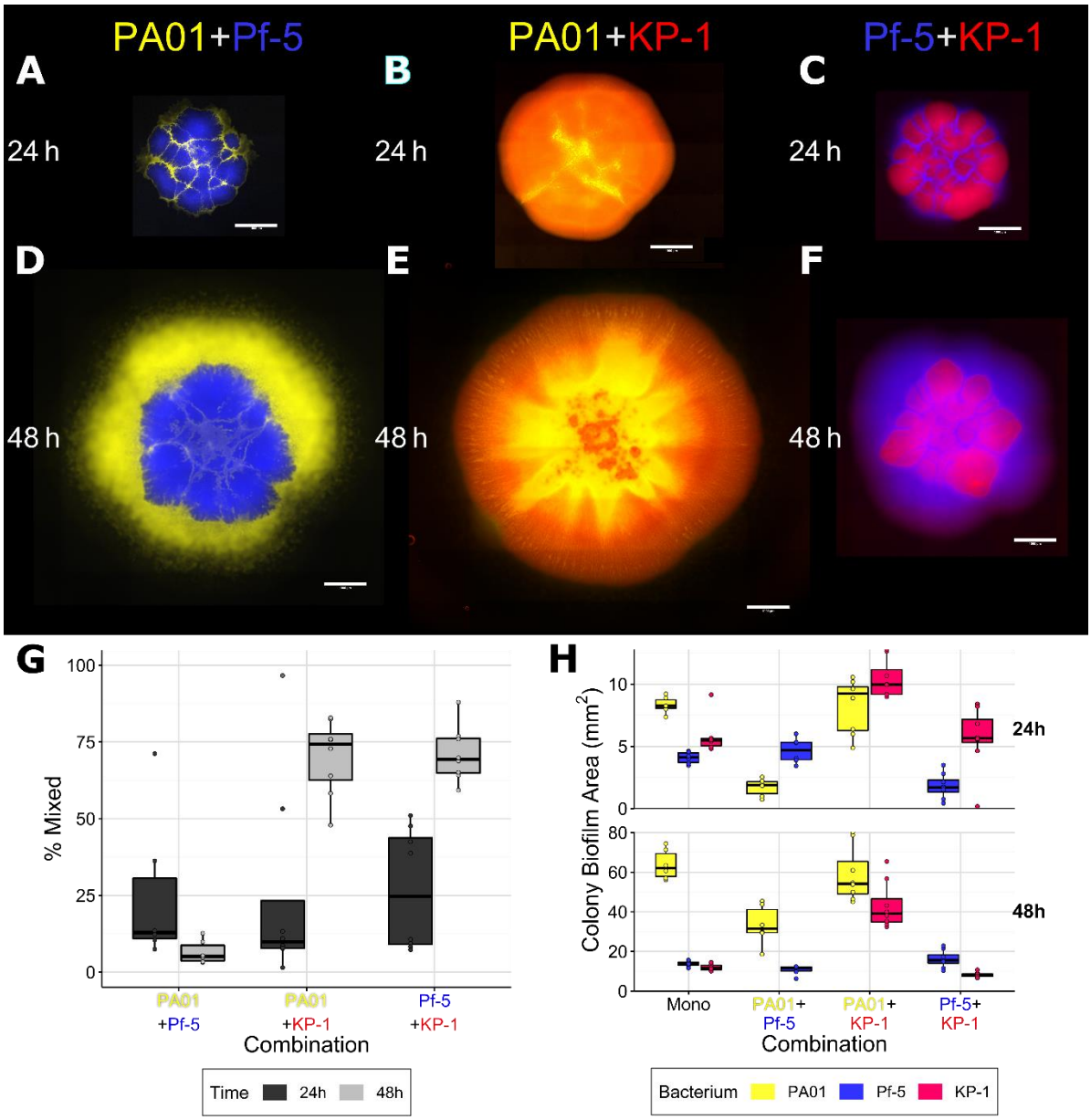

Figure 2: Dual species colony biofilms of *P. aeruginosa* PAO1 and *P. protegens* Pf-5 (A, D), *P. aeruginosa* PAO1 and *K. pneumoniae* KP-1 (B, E), and *P. protegens* Pf-5 and *K. pneumoniae* KP-1 (C, F), overlap between differently labeled strains (G) and the area covered by individual species in colony biofilms (H). Each species was labeled with different fluorescent protein genes and are presented here as yellow (*P. aeruginosa* PAO1), blue (*P. protegens*) and red (*K. pneumoniae*). Strains were mixed 1:1 at the time of inoculation and colonies were imaged after 24 and 48 h of growth. Scale bar indicates 1000 µm. Boxplots are presented in Tukey style. Colony area was quantified manually ($n \geq 6$).

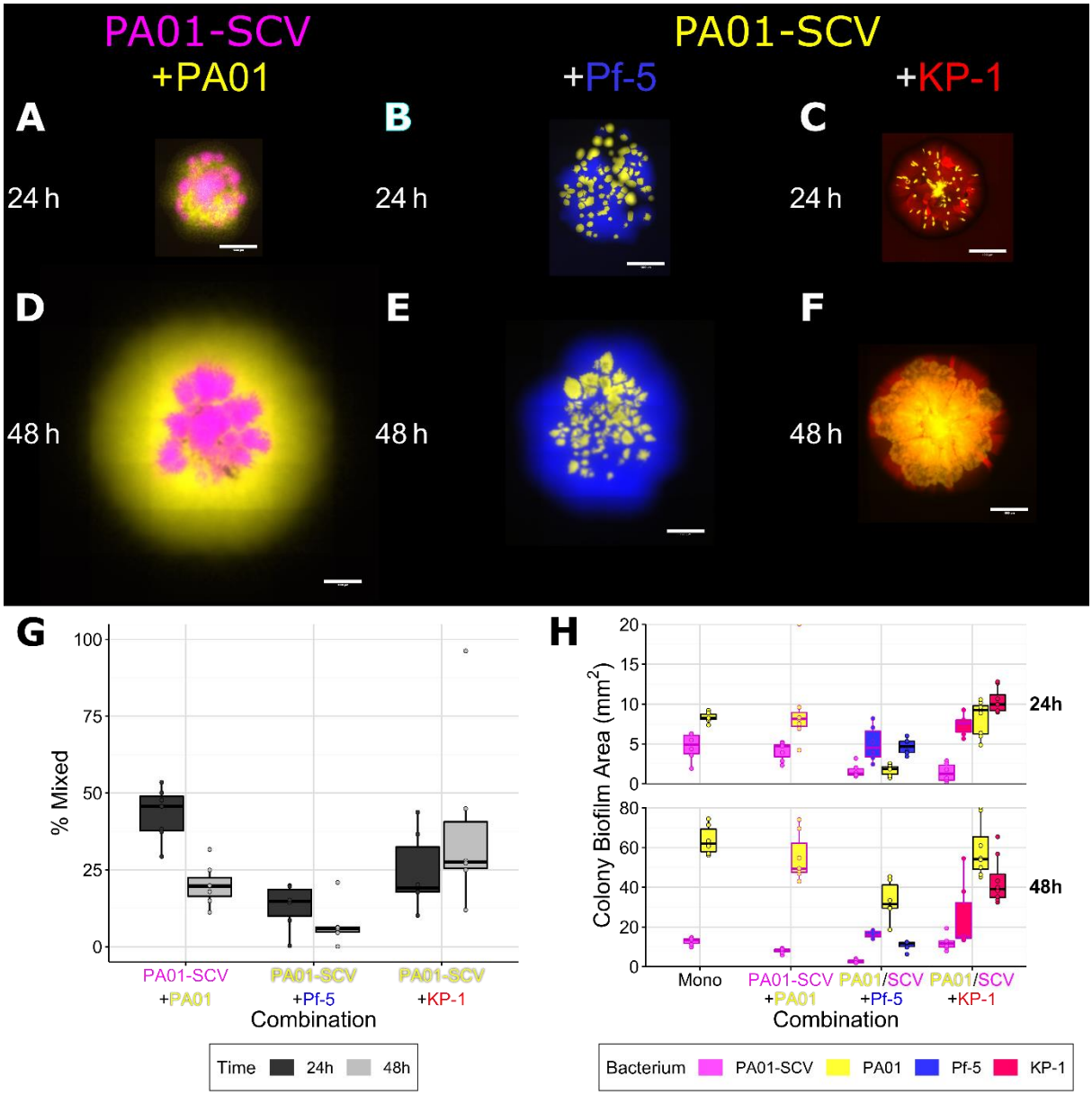

Figure 3: Co-culture colony biofilms consisting of *P. aeruginosa* PAO1 and *P. aeruginosa* PAO1 small colony variant (SCV) (A, D), *P. aeruginosa* PAO1 SCV and *P. protegens* Pf-5 (B, E) and *P. aeruginosa* PAO1 SCV and *K. pneumoniae* KP-1 (C, F), overlap between differently labeled strains (G), and area covered by individual species/strains (H). Each species was labeled with different fluorescent protein genes and are presented here as yellow (*P. aeruginosa* wild-type when paired with the SCV, SCV when paired with the other two species), magenta (*P. aeruginosa* SCV), blue (*P. protegens*) and red (*K. pneumoniae*). Strains were mixed 1:1 at the time of inoculation and colonies were imaged after 24 and 48 h of growth. Scale bar indicates 1000 µm. Boxplots are presented in Tukey style. Colony area was quantified manually ($n \geq 6$). For the area boxplots (H) combinations of *P. aeruginosa* with *P. protegens* or *K. pneumoniae*, boxes outlined in black represent the wild-type (same data as Figure 2, H), outlines in magenta represent combinations with the SCV.

Co-cultures with a *P. aeruginosa* Small Colony Variant

To investigate the effect of the type IV pilus (TFP) of *P. aeruginosa* in colony biofilms, a small colony variant (SCV) was cultured in dual species biofilms with the parental strain, *P. protegens* and *K. pneumoniae*. The SCV has a mutation in *pilT* preventing pilus retraction and therefore TFP motility [32]. Colonies formed with the SCV differed from those with wild-type *P. aeruginosa* and the mixing of strains/species also differed (Figure 3). Both *P. aeruginosa* and *P. protegens* formed a perimeter around the SCV, but there was no mixing of strains/species. Mixing of the SCV and *K. pneumoniae* was ~25%, even at 48 h when they visually appeared to be almost completely overlapping. Closer inspection indicated this was due to the high fluorescence intensity of the SCV relative to the *K. pneumoniae* tagged with dsRed resulting in many bins near, but above the mixing threshold of 0.25. When mixing was calculated by thresholding the individual channels (Supplementary Figure 3), 75% of SCV and *K. pneumoniae* colony area was mixed. The SCV colonized less area than wild-type *P. aeruginosa*, ~12 mm^2 compared to ~70 mm^2, respectively, at 48 h (Figure 3, H). In dual species biofilms, the area covered by the SCV was reduced to ~2 mm^2 at 48 h in the presence of *P. protegens*. When grown with *K. pneumoniae*, the SCV covered less area at 24 h but this was not apparent at 48 h. The SCV did not affect the area covered by the other strains and in contrast to when the parental strain of *P. aeruginosa* was present, the SCV did not increase the area covered by *K. pneumoniae*.

Co-cultures with a Non-Mucoid *K. pneumoniae* Variant

To investigate the effects of extracellular matrix (ECM) production by *K. pneumoniae*, a non-mucoid variant (NMV) was cultured in dual strain/species biofilms with the parental strain, *P. aeruginosa* and *P. protegens*. The NMV has a mutation in a putative UDP-glucose lipid transferase located within a probable colanic acid synthesis gene cluster, preventing it from producing its normal, thick ECM [32]. Single-strain colonies formed by the NMV differed from wild-type *K. pneumoniae* (Supplementary Figure 4). Boundaries between sectors of the NMV were jagged instead of straight as was observed for the wild-type. Dual-species colonies with the NMV also differed as it did not mix with wild-type *K. pneumoniae* or *P. protegens* (Figure 4). When grown with *P. aeruginosa*, mixing was lower at 48 h compared to 24 h. When grown as single strain biofilms, wild-type *K. pnenumoniae* and the NMV covered a similar area. When the two were co-cultured together, the NMV covered less area, ~4 mm^2, compared to when grown alone, ~12 mm^2, at 24 h, but there was no change at 48 h. The area covered by the NMV was also decreased when paired with *P.*

protegens, however, neither of these differences persisted at 48 h. In contrast, the area covered by *P. aeruginosa* was decreased when grown in the presence of the *K. pneumoniae* NMV at 24 h but not 48 h. When paired with *P. aeruginosa*, the area covered by the NMV was not significantly increased as was observed for the parental *K. pneumoniae* strain when paired with *P. aerguinosa*.

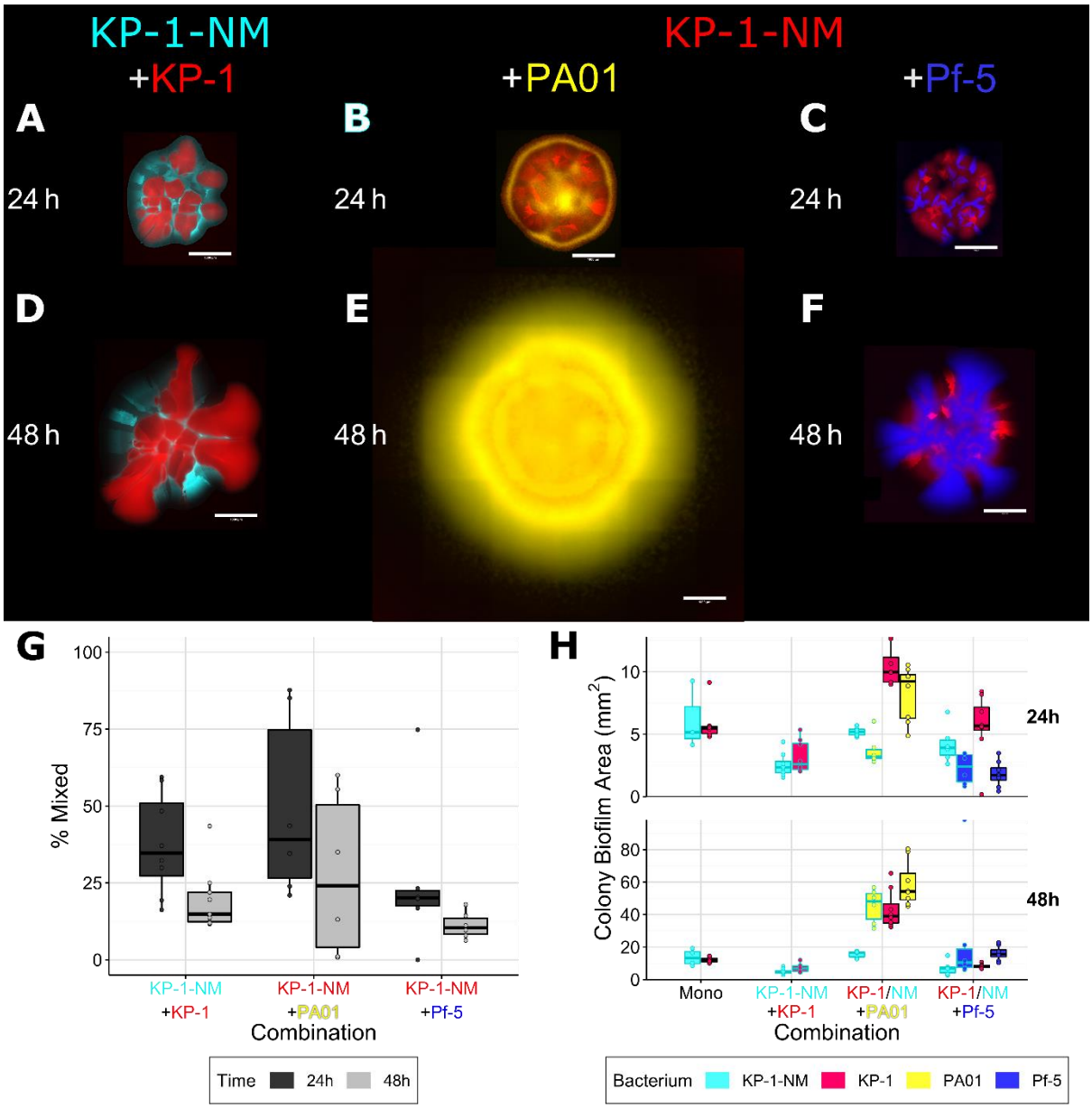

Figure 4: Co-culture colony biofilms consisting of *K. pneumoniae* KP-1 with the *K. pneumoniae* KP-1 non-mucoid variant (NMV) (A, D), *K. pneumoniae* KP-1 NMV with *P. protegens* Pf-5 (B, E), and *K. pneumoniae* KP-1 NMV with *P. aeruginosa* PAO1 (C, F), overlap between differently labeled strains (G) and area covered by individual species/strains (H). Each species was labeled with a different fluorescent protein gene and are presented here as yellow (*P. aeruginosa*), blue (*P. protegens*), red (*K. pneumoniae* wild-type when paired

with the NMV, *K. pneumoniae* NMV when paired with the other species) and cyan (*K. pneumoniae* NMV). Strains were mixed 1:1 at the time of inoculation and colonies were imaged after 24 and 48 h of growth. Scale bar indicates 1000 µm. Boxplots are presented in Tukey style. Colony area was quantified manually (n ≥ 6). For the area boxplots (H), combinations of *K. pneumoniae* with *P. aeruginosa* or *P. protegens*, boxes outlined in black represent the wild-type (same data as Figure 2, H), outlines in cyan represent the NMV.

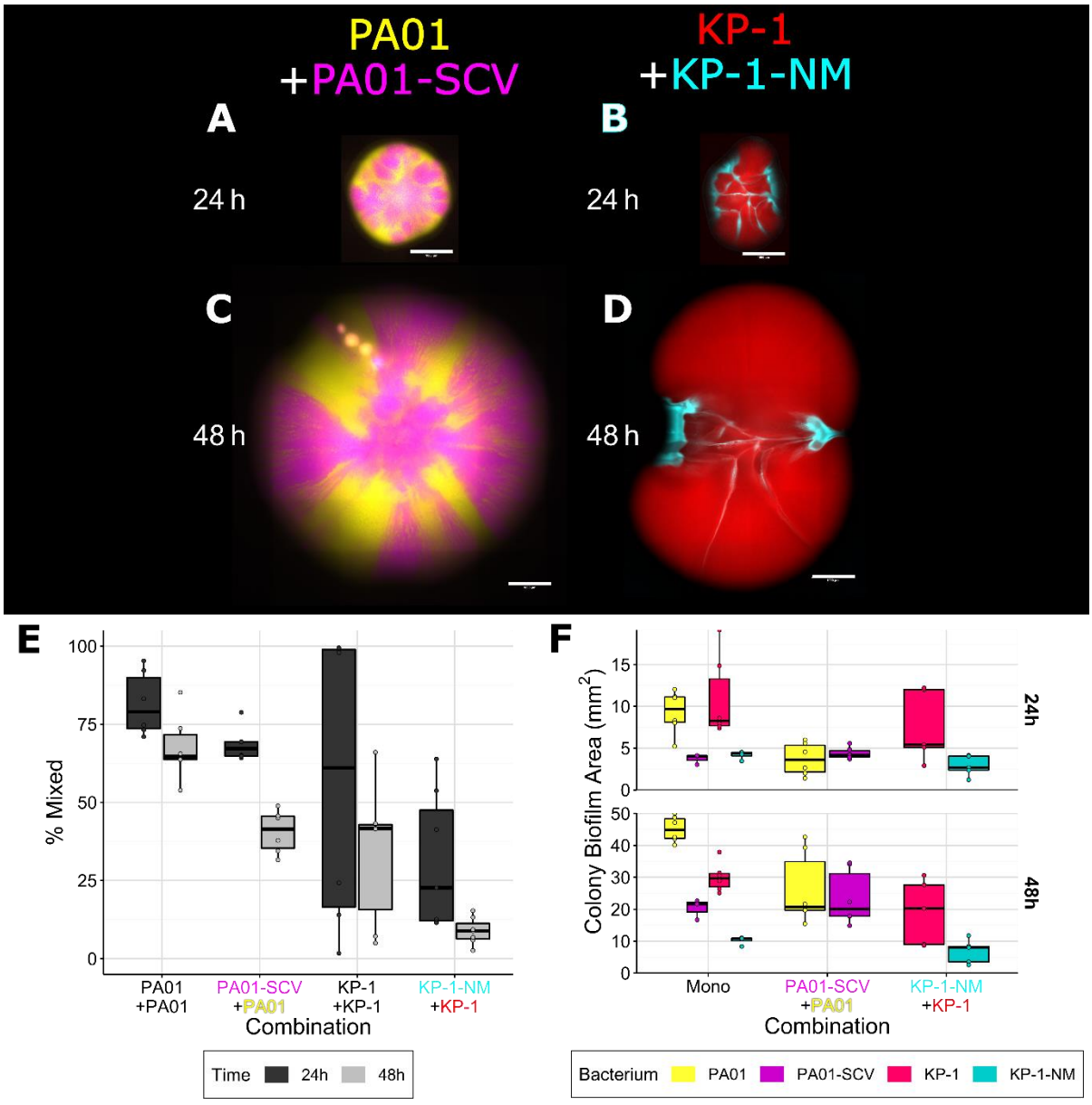

Figure 5: Co-culture colony biofilms consisting of *P. aeruginosa* PAO1 with *P. aeruginosa* small colony variant (SCV) (A, C), and *K. pneumoniae* with *K. pneumoniae* KP-1 non-mucoid variant (NMV) (B, D), overlap between differently labeled strains (E) and area covered by individual species/strains (F). Each species was labeled with different fluorescent protein gene and are presented here as yellow (*P. aeruginosa* wild-type), magenta (*P.*

aeruginosa SCV), red (*K. pneumoniae* wild-type) and cyan (*K. pneumoniae* NMV). Strains were mixed 1:1 at the time of inoculation and colonies were imaged after 24 and 48 h of growth. Scale bar indicates 1000 µm. was calculated from raw images ($n \geq 6$). Boxplots are Tukey style. Colony area was quantified manually ($n \geq 4$).

Colony Biofilms Grown on 0.6% Agar

The percentage of agar influences motility, as lower percentages enable swarming and/or swimming motility and affect the colony growth of highly mucoid strains [25]. Growth on lower percentage agar was thus expected to affect intraspecies interactions between the wild-type strains of *P. aeruginosa* and *K. pneumoniae* and their non-motile (SCV) and non-mucoid (NMV) variants. Colony biofilms consisting of wild-type and mutant strains grown on 0.6% agar had altered morphologies (Figure 5), but those consisting of two differently labeled wild-type strains did not, and did not separate into sectors any differently (Supplementary Figure 5). When the *P. aeruginosa* SCV was co-cultured with its parental strain, both strains expanded outwards together, but were less mixed (~35% at 48 h) compared to the two differently coloured wild-type *P. aeruginosa* strains (~65% at 48 h, Figure 1G), which was also lower than that observed on 1.5% agar (75%, Figure 1, G). When the *K. pneumoniae* NMV was co-cultured with the wild-type, the two strains were not mixed, however by 48 h the wild-type had expanded much more than the NMV (Figure 5, E). When two wild-type *K. pneumoniae* strains were grown together, they were more mixed (~40% at 48 h), than when grown on 1.5% agar (25%, Figure 1, G and Table 2). The colony area was significantly higher for the *P. aeruginosa* SCV on 0.6% compared to 1.5% agar at 48 h (~20 vs ~10 mm^2). This was significantly lower than the wild-type on 0.6% agar (~50 mm^2), which was also significantly decreased compared to on 1.5% agar (~70 mm^2). While there appeared to be a difference between colony area of both the wild-type and SCV between when they were cultured alone vs. together, this difference was not significant. The *K. pneumoniae* wild-type colonized a significantly increased area on 0.6% agar (~27 mm^2) compared to the NMV (~10 mm^2) and the wild-type on 1.5% agar (~11 mm^2). When they were co-cultured, the area colonized by the wild-type and NMV was significantly lower only at 24 h.

Table 2: Comparison of effects of 0.6% agar on colony biofilms of *P. aeruginosa*, *P. aeruginosa* small colony variant (SCV), *K. pneumoniae* and *K. pneumoniae* non-mucoid (NM) variant.

	Wild-type compared to mutant				**Monospecies 0.6% agar**		**Wild-type and mutant 0.6% agar**	
	1.5% Agar		**0.6% Agar**					
Time	24 h	48 h	24 h	48 h	24 h	48 h	24 h	48 h
PAO1	**SCV ↓**	**SCV ↓**	**SCV ↓**	**SCV ↓**		↓		
PAO1-SCV						↑		
KP-1			**WT ↑**	**WT ↑**		↑	↓	
KP-1-NMV							↓	

* Results from comparisons between the wild-type and mutant on each percentage of agar, between agar percentages for each strain and the between cultivation alone or in combination are shown. Interactions that resulted in a significant increase in area are indicated by ↑ and decreases by ↓, using analysis of variance and Tukey's honest significant differences post-hoc test. Differences were considered significant if their multiple-testing adjusted p-value (95% confidence) was below 0.05. Empty cells indicate no significant change.

Discussion

Colony biofilms highlight differences in intraspecies interactions

For each of the three species from our model community, intraspecific competition resulted in species specific patterns of sector formation. Separation of mixed colonies into sectors has been attributed to genetic drift at the leading edge of the biofilm, as despite having equal fitness, stochastic effects result in new territory being colonized by either one strain or the other, but not both [38]. Here we show that the shape of the boundaries between sectors depends on the bacterium's physiological traits. The separation of wild-type *K. pneumoniae* strains into sectors with straight boundaries resembled that of *Saccharomyces*

cerevisiae [22], whereas the jagged boundaries of *P. protegens* were more similar to those of *P. stutzeri* [24], simulated rod-shaped cells [39] or *E. coli* [38]. In the case of *E. coli*, the formation of fractal boundaries between sectors has been explained by the anisotropic forces of cell division and growth causing unlinked chains of rod-shaped cells to buckle [40]. Thus, similar buckling likely causes the formation of jagged edges between boundaries of the wild-type *P. protegens* strains. The jagged boundaries visible between sectors within *K. pneumoniae* NMV colonies indicate that its secreted extracellular matrix (ECM) causes the straight boundaries between sectors observed in the wild-type. Colony biofilms of *P. aeruginosa* grown on nutrient rich LB medium were previously shown to be well mixed [41], similar to our observations here using minimal medium. The observation that *pilB* mutants segregate into clear sectors [41] and the resemblance of videos of the edge of *P. aeruginosa* biofilms (Supplementary Video 1) to those showing TFP motility [42] indicates that this motility likely enabled the mixing of the *P. aeruginosa* wild-type strains.

Table 3: Comparison of dual species interactions for *P. aeruginosa*, *P. aeruginosa* small colony variant (SCV), *P. protegens*, *K. pneumoniae* and *K. pneumoniae* non-mucoid variant (NMV).

Affects / Bacterium	*P. aeruginosa*	*P. aeruginosa* SCV	*P. protegens*	*K. pneumoniae*	*K. pneumoniae* NMV
P. aeruginosa				↑	
P. aeruginosa-SCV	↓				ND
P. protegens	↓	↓		↓	
K. pneumoniae					↓
K. pneumoniae-NMV		ND			

***** Empty cells indicates no difference between single and dual species biofilm was observed, ND indicates a combination which was not determined. Interactions that resulted in a significant increase in area are indicated by ↑and decreases by ↓ compared to the monospecies biofilm by analysis of variance and Tukey's honest significant differences post-hoc test. Differences were considered significant if their multiple-testing adjusted p-value was below 0.05 for 48 h comparisons.

Interspecies interactions differ from intraspecies interactions

To refer to the observed differences in spatial distribution, we use the term 'biofilm community morphology' or more simply, 'community morphology', to align with community function and community composition within these colony biofilms. Previous studies have focused on either identical, but differently labeled strains, or strains with specific genetic modifications, while here, we investigated interactions between different species. While our single strain data match published data, it is clear here that community morphologies of mixed species biofilms differ markedly. Thus, the data presented here show how the different physiological traits of the three studied bacteria determine community morphology and composition.

We have assessed the three pairwise interactions tested here using the notation of Momeni et al. [21], where A [~,~] B indicates a neutral interaction and A[↑,↓]B indicates a relationship where A benefits and B is negatively affected (Table 3). The community morphology of *P. aeruginosa* with *P. protegens*, and *P. protegens* with *K. pneumoniae* are similar as one strain expanded outward faster and surrounded the other. Although the area covered by the inner strains was not reduced compared to when they were grown alone, both interactions negatively affect the inner strain as it no longer had equal access to space/nutrients. For the first pair, the area covered by the outer strain, *P. aeruginosa*, was significantly decreased, indicating that both strains experienced negative outcomes from the interaction, so *P. aeruginosa* [↓,↓] *P. protegens*. For the second pair, *P. protegens* was the outer strain but its area was not reduced so, *P. protegens* [~,↓] *K. pneumoniae*. In the third case, when *P. aeruginosa* was paired with *K. pneumoniae*, *P. aeruginosa* did not differ in the amount of area covered but *K. pneumoniae* received a significant benefit, so, *P. aeruginosa* [~,↑] *K. pneumoniae*.

Mixing was observed between both *Pseudomonas* species when they were grown as dual species biofilms with *K. pneumoniae* (Figure 2, G), but this translated to a benefit for *K. pneumoniae* only with *P. aeruginosa*. In strains of *E. coli* engineered to have equal growth rates but different cell shapes, small cells were found on top of the biofilm colonies and larger cells were below, at the agar surface where they maintained access to nutrients obtained from an agar surface [23]. *K. pneumoniae* cells are larger than *Pseudomonas* which may have allowed *P. protegens* to overgrow it and prevent *K. pneumoniae* from expanding further. Even though they have similarly sized cells, *P. aeruginosa* was able to move, expand in surface area and colonize space faster than *P. protegens*, likely due to its type IV pilus (TFP) enabled twitching motility.

P. aeruginosa twitching motility is important for interactions

Twitching motility by *P. aeruginosa* has been best studied in interstitial biofilms, in between an agar surface and a glass coverslip [42–45]. The colony biofilms studied here appear qualitatively similar, although the expanding front does not form intricate lattices. Without a functional TFP, the SCV could only colonize about 1/5 the area of the wild-type. When paired with wild-type *P. aeruginosa* or *P. protegens*, the SCV was outcompeted for space, indicating that TFP motility is a competitive trait. It also appears to be a cooperative trait as the area colonized by *K. pneumoniae* was not increased when paired with the *P. aeruginosa* SCV, whereas it was increased three-fold when paired with TFP motile, wild-type *P. aeruginosa*. In flow-cell biofilms, a *pilA* mutant of *P. aeruginosa* was less competitive with *Agrobacterium tumefaciens* [46], but conversely, outcompeted *Staphylococcus aureus* [47]. Motility, as a competitive trait, has been suggested to allow strains better access nutrients, to cover other organisms or to disrupt their biofilms [48], which is supported by our results. Even though *P. aeruginosa* was able to cover *K. pneumoniae* with and without a functional TFP, only the motile wild-type *P. aeruginosa* had a commensal relationship with *K. pneumoniae*, indicating that motility can also be a cooperative trait.

K. pneumoniae secreted matrix is important for interactions

Self-secreted ECM is a hallmark of biofilms that influences the spatial positioning and interactions between cells within a biofilm [20]. Matrix secretion allows producing cells to better access nutrients in colony biofilms of *P. fluorescens* [49] and for simulated cells under flow conditions [50], by excluding other cells. In flow-cell biofilms, *K. pneumoniae* NMV outcompeted its isogenic wild-type strain, but was less fit when grown with *P. aeruginosa* and *P. protegens* [32]. In colony biofilms, the *K. pneumoniae* NMV colonized the same total area as its parental, wild-type strain when alone, but did not mix with the wild-type when the two were co-cultured. Furthermore, the NMV did not colonize more area when paired with *P. aeruginosa* and was outcompeted by *P. protegens*, resulting in less area covered compared to the NMV when grown as a monospecies biofilm. This indicates that the ECM normally produced by *K. pneumoniae* KP-1 improves interspecies, but not intraspecies, competition. The mutual exclusion observed between the wild-type and NMV also indicates that the NMV cannot take advantage of the wild-type, similarly to exclusion by *B. subtilis* [51] and *V. cholerae* [52].

Agar concentration changes inter-strain interaction outcomes

It is well understood that agar concentration influences bacterial motility [53]. It also affects the ability of biofilms to extract nutrients as it determines the osmotic pressure of an environment [25]. Here we showed that lowering the agar concentration from 1.5% to 0.6% allowed the TFP motility deficient SCV of *P. aeruginosa* to colonize as much area as the wild-type and was not encircled by the parental wild-type when they were co-cultured (Table 3). Conversely, the *K. pneumoniae* NMV was less effective at colonization on 0.6% agar compared to the wild-type, but was still able to compete with the wild-type when co-cultured. For the *P. aeruginosa* SCV, lowering the agar concentration likely enabled flagella-based motility that could compensate for the defect in twitching motility. Motility is important for colonization of roots [54], the gastrointestinal tract of Zebra fish [55] and for the persistence of uropathogenic *E. coli* [56]. Here, we showed that motility influenced intraspecies competition but the outcome depended on environmental conditions. Previously, we observed that the *P. aeruginosa* SCV completely outcompeted wild-type *P. aeruginosa* in flow cell biofilms [32]. The increased attachment provided by hyper-piliation of the SCV [44, 57] likely provides this benefit in flow cells, whereas the lack of motility was a detriment in colony biofilms. This highlights the differences in environmental pressures between the two kinds of biofilm. Hyper-piliation also leads to aggregation [58], which may explain how the *P. aeruginosa* wild-type and SCV separated into sectors with straight boundaries on 0.6% agar. This appeared to be similar to the differently tagged strains of *K. pneumoniae*, indicating that this community morphology may not exclusively be caused by matrix secretion.

For *K. pneumoniae*, lowering the agar concentration allowed the wild-type to colonize more area, which was similar to how a rugose strain of *V. cholerae* that hypersecretes ECM formed larger colonies on lower concentrations of agar [25]. In *V. cholerae*, it was demonstrated that matrix secretion generates an osmotic pressure gradient between the agar and the biofilm, allowing the biofilm to expand by physical swelling and increased nutrient uptake. It is likely that this is a general mechanism attributable to the biofilm matrix. In this context, the wild-type *K. pneumoniae* would be similar to the rugose *V. cholerae*, producing larger amounts of ECM, while the *K. pneumoniae* NMV and wild-type *V. cholerae* are analogous in their relatively lower amount of ECM production. The community morphology of dual strain biofilms of ECM secretors and non-secretors differed between the two species. In *V. cholerae*, the hyper-secretor was encircled by the non-secretor at both 1.5 and 0.6% agar, but colonized far more area at 0.6% as the non-secretor was pushed to the outside of the

colony. Conversely, the *K. pneumoniae* NMV was not displaced and even prevented spreading by wild-type *K. pneumoniae* (Figure 5, D). Similar to *V. cholerae*, the *K. pneumoniae* NMV did not benefit from the matrix secreted by wild-type *K. pneumoniae* as its area was not increased in co-culture. In *B. subtilis*, it was also observed that ECM-producing cells outcompete non-secretors [26], and to a higher degree when the humidity is higher (which is similar to lower agar concentration). Also, osmotic pressure generated by the ECM enhances colony biofilm spreading [59]. Thus, matrix production appears to be a general strategy of bacteria that increases competitiveness of species in colony biofilms.

Conclusions

Interactions between bacteria are key for determining the composition and function of communities. Here we used colony biofilms to investigate intra- and inter-species interactions. Using the members of our three species model community, we showed that they differ in how they interact with members of their own species due to their physiological traits: TFP motility in *P. aeruginosa* allowed populations to mix whereas ECM in *K. pneumoniae* caused straight borders between population sectors. Using mutants deficient in these traits we showed that their impact depended on the agar concentration. These physiological traits were also important when interspecies interactions in colony biofilms were examined. The motility of *P. aeruginosa* enables it to outcompete *P. protegens* and to facilitate increased colonization area by *K. pneumoniae*. Importantly, the spatial distribution of species, the "community morphology", observed for dual-species colony biofilms did not resemble any patterns previously seen for experimental or simulated monospecies and dual-strain colony biofilms. These experiments show that interspecies interactions are more complex than intraspecies interactions as differences in physiology have a large influence on the outcome and community morphology determined using colony biofilms is a powerful way to investigate these interactions.

Acknowledgments

The authors would like to thank Sujatha Subramoni for helpful advice regarding the three species community, Talgat Sailov for microscopy assistance and Diane MacDougald for reading the manuscript and providing helpful comments.

Conflict of Interest

The authors state that they have no conflict of interest.

References

1. Elias S, Banin E. Multi-species biofilms: living with friendly neighbors. *FEMS Microbiol Rev* 2012; **36**.

2. Rendueles O, Ghigo J-M. Multi-species biofilms: how to avoid unfriendly neighbors. *FEMS Microbiol Rev* 2012; **36**: 972–989.

3. Ghoul M, Mitri S. The Ecology and Evolution of Microbial Competition. *Trends Microbiol* . 2016.

4. Morris BEL, Henneberger R, Huber H, Moissl-Eichinger C. Microbial syntrophy: interaction for the common good. *FEMS Microbiol Rev* 2013; **37**: 384–406.

5. Cornforth DM, Foster KR. Antibiotics and the art of bacterial war. *Proc Natl Acad Sci U S A* 2015; **112**: 10827–8.

6. Sharma A, Inagaki S, Sigurdson W, Kuramitsu HK. Synergy between Tannerella forsythia and Fusobacterium nucleatum in biofilm formation. *Oral Microbiol Immunol* 2005; **20**: 39–42.

7. Yamada M, Ikegami A, Kuramitsu HK. Synergistic biofilm formation by *Treponema denticola* and *Porphyromonas gingivalis*. *FEMS Microbiol Lett* 2005; **250**: 271–277.

8. Gonzalez D, Sabnis A, Foster KR, Mavridou DAI. Costs and benefits of provocation in bacterial warfare. *Proc Natl Acad Sci U S A* 2018; 201801028.

9. Cordero OX, Datta MS. Microbial interactions and community assembly at microscales. *Curr Opin Microbiol* 2016; **31**: 227–234.

10. Abreu NA, Taga ME. Decoding molecular interactions in microbial communities. *FEMS Microbiol Rev* 2016; **40**: 648–663.

11. Madsen JS, Sørensen SJ, Burmølle M. Bacterial social interactions and the emergence of community-intrinsic properties. *Curr Opin Microbiol* 2018; **42**: 104–109.

12. Foster KR, Bell T. Competition, not cooperation, dominates interactions among culturable microbial species. *Curr Biol* 2012.

13. Russel J, Røder HL, Madsen JS, Burmølle M, Sørensen SJ. Antagonism correlates with metabolic similarity in diverse bacteria. *Proc Natl Acad Sci U S A* 2017; **114**: 10684–10688.

14. Ren D, Madsen JS, Sørensen SJ, Burmølle M. High prevalence of biofilm synergy among bacterial soil isolates in cocultures indicates bacterial interspecific cooperation. *ISME J* 2015; **9**: 81–89.

15. Burmølle M, Webb JS, Rao D, Hansen LH, Sørensen SJ, Kjelleberg S. Enhanced biofilm formation and increased resistance to antimicrobial agents and bacterial invasion are caused by synergistic interactions in multispecies biofilms. *Appl Environ Microbiol* 2006; **72**: 3916–23.

16. Tan CH, Lee KWK, Burmølle M, Kjelleberg S, Rice SA. All together now: experimental multispecies biofilm model systems. *Environ Microbiol* 2017; **19**: 42–53.

17. Røder HL, Sørensen SJ, Burmølle M. Studying Bacterial Multispecies Biofilms: Where to Start? *Trends Microbiol* 2016; **24**: 503–513.

18. Dragoš A, Kiesewalter H, Martin M, Hsu C-Y, Hartmann R, Wechsler T, et al. Division of Labor during Biofilm Matrix Production. *Curr Biol* 2018; **28**: 1903–1913.e5.

19. Lee KWK, Periasamy S, Mukherjee M, Xie C, Kjelleberg S, Rice SA. Biofilm development and enhanced stress resistance of a model, mixed-species community biofilm. *ISME J* 2014; **8**: 894–907.

20. Nadell CD, Drescher K, Foster KR. Spatial structure, cooperation and competition in biofilms. *Nat Rev Microbiol* 2016.

21. Momeni B, Brileya KA, Fields MW, Shou W. Strong inter-population cooperation leads to partner intermixing in microbial communities. *Elife* 2013; **2**.

22. Müller MJI, Neugeboren BI, Nelson DR, Murray AW. Genetic drift opposes mutualism during spatial population expansion. *Proc Natl Acad Sci U S A* 2014; **111**: 1037–42.

23. Smith WPJ, Davit Y, Osborne JM, Kim W, Foster KR, Pitt-Francis JM. Cell morphology drives spatial patterning in microbial communities. *Proc Natl Acad Sci U S A* 2017; **114**: E280–E286.

24. Goldschmidt F, Regoes RR, Johnson DR. Successive range expansion promotes diversity and accelerates evolution in spatially structured microbial populations. *ISME J* 2017; **11**: 2112–2123.

25. Yan J, Nadell CD, Stone HA, Wingreen NS, Bassler BL. Extracellular-matrix-mediated osmotic pressure drives Vibrio cholerae biofilm expansion and cheater exclusion. *Nat Commun* 2017; **8**: 327.

26. van Gestel J, Weissing FJ, Kuipers OP, Kovács ÁT. Density of founder cells affects spatial pattern formation and cooperation in Bacillus subtilis biofilms. *ISME J* 2014; **8**: 2069–2079.

27. Frost I, Smith WPJ, Mitri S, Millan AS, Davit Y, Osborne JM, et al. Cooperation, competition and antibiotic resistance in bacterial colonies. *ISME J* 2018; **12**: 1582–1593.

28. Ramette A, Frapolli M, Saux MF Le, Gruffaz C, Meyer JM, Défago G, et al. Pseudomonas protegens sp. nov., widespread plant-protecting bacteria producing the biocontrol compounds 2,4-diacetylphloroglucinol and pyoluteorin. *Syst Appl Microbiol* 2011.

29. Lim CK, Hassan KA, Penesyan A, Loper JE, Paulsen IT. The effect of zinc limitation on the transcriptome of *Pseudomonas protegens* Pf-5. *Environ Microbiol* 2013; **15**: 702–715.

30. Chazal PM. Pollution of modern metalworking fluids containing biocides by pathogenic bacteria in France. *Eur J Epidemiol* 1995; **11**: 1–7.

31. Anand AAP, Vennison SJ, Sankar SG, Prabhu DIG, Vasan PT, Raghuraman T, et al. Isolation and Characterization of Bacteria from the Gut of *Bombyx mori* that Degrade Cellulose, Xylan, Pectin and Starch and Their Impact on Digestion. *J Insect Sci* 2010; **10**: 1–20.

32. Kelvin Lee KW, Hoong Yam JK, Mukherjee M, Periasamy S, Steinberg PD, Kjelleberg S, et al. Interspecific diversity reduces and functionally substitutes for intraspecific variation in biofilm communities. *ISME J* 2016; **10**: 846–857.

33. Peng T, Thorn K, Schroeder T, Wang L, Theis FJ, Marr C, et al. A BaSiC tool for background and shading correction of optical microscopy images. *Nat Commun* 2017; **8**: 14836.

34. Preibisch S, Saalfeld S, Tomancak P. Globally optimal stitching of tiled 3D microscopic image acquisitions. *Bioinformatics* 2009; **25**: 1463–5.

580 35. Schneider CA, Rasband WS, Eliceiri KW. NIH Image to ImageJ: 25 years of image
581 analysis. *Nat Methods* 2012; **9**: 671–675.

582 36. Barthelme S. imager: Image Processing Library Based on 'CImg'. 2018.
583 https://CRAN.R-project.org/package=imager.

584 37. Landini G, Randell DA, Fouad S, Galton A. Automatic thresholding from the
585 gradients of region boundaries. *J Microsc* 2017; **265**: 185–195.

586 38. Hallatschek O, Hersen P, Ramanathan S, Nelson DR. Genetic drift at expanding
587 frontiers promotes gene segregation. *Proc Natl Acad Sci U S A* 2007; **104**: 19926–30.

588 39. Blanchard AE, Lu T. Bacterial social interactions drive the emergence of differential
589 spatial colony structures. *BMC Syst Biol* 2015; **9**: 59.

590 40. Rudge TJ, Federici F, Steiner PJ, Kan A, Haseloff J. Cell Polarity-Driven Instability
591 Generates Self-Organized, Fractal Patterning of Cell Layers. *ACS Synth Biol* 2013; **2**:
592 705–714.

593 41. Mitri S, Clarke E, Foster KR. Resource limitation drives spatial organization in
594 microbial groups. *ISME J* 2016; **10**: 1471–1482.

595 42. Gloag ES, Turnbull L, Huang A, Vallotton P, Wang H, Nolan LM, et al. Self-
596 organization of bacterial biofilms is facilitated by extracellular DNA. *Proc Natl Acad*
597 *Sci U S A* 2013; **110**: 11541–6.

598 43. Semmler ABT, Whitchurch CB, Mattick JS. A re-examination of twitching motility in
599 Pseudomonas aeruginosa. *Microbiology* 1999; **145**: 2863–2873.

600 44. Whitchurch CB, Mattick JS. Characterization of a gene, pilU, required for twitching
601 motility but not phage sensitivity in Pseudomonas aeruginosa. *Mol Microbiol* 1994;
602 **13**: 1079–1091.

603 45. Turnbull L, Toyofuku M, Hynen AL, Kurosawa M, Pessi G, Petty NK, et al. Explosive
604 cell lysis as a mechanism for the biogenesis of bacterial membrane vesicles and
605 biofilms. *Nat Commun* 2016; **7**: 11220.

606 46. An D, Danhorn T, Fuqua C, Parsek MR. Quorum sensing and motility mediate
607 interactions between Pseudomonas aeruginosa and Agrobacterium tumefaciens in
608 biofilm cocultures. *Proc Natl Acad Sci* 2006; **103**: 3828–33.

609 47. Yang L, Liu Y, Markussen T, Høiby N, Tolker-Nielsen T, Molin S. Pattern
610 differentiation in co-culture biofilms formed by *Staphylococcus aureus* and
611 *Pseudomonas aeruginosa*. *FEMS Immunol Med Microbiol* 2011; **62**: 339–347.

612 48. Rendueles O, Ghigo J-M. Mechanisms of competition in biofilm communities.
613 *Microbiol Spectr* 2015; **3**.

614 49. Kim W, Racimo F, Schluter J, Levy SB, Foster KR. Importance of positioning for
615 microbial evolution. *Proc Natl Acad Sci U S A* 2014; **111**: E1639-47.

616 50. Jayathilake PG, Jana S, Rushton S, Swailes D, Bridgens B, Curtis T, et al.
617 Extracellular Polymeric Substance Production and Aggregated Bacteria Colonization
618 Influence the Competition of Microbes in Biofilms. *Front Microbiol* 2017; **8**: 1865.

619 51. Martin M, Dragoš A, Hölscher T, Maróti G, Bálint B, Westermann M, et al. De novo
620 evolved interference competition promotes the spread of biofilm defectors. *Nat*
621 *Commun* 2017; **8**: 15127.

622 52. Nadell CD, Drescher K, Wingreen NS, Bassler BL. Extracellular matrix structure
623 governs invasion resistance in bacterial biofilms. *ISME J* 2015; **9**: 1700–1709.

624 53. Greenberg EP, Canale-Parola E. Motility of flagellated bacteria in viscous
625 environments. *J Bacteriol* 1977; **132**: 356–8.

626 54. Pliego C, de Weert S, Lamers G, de Vicente A, Bloemberg G, Cazorla FM, et al. Two
627 similar enhanced root-colonizing *Pseudomonas* strains differ largely in their
628 colonization strategies of avocado roots and *Rosellinia necatrix* hyphae. *Environ*
629 *Microbiol* 2008; **10**: 3295–3304.

630 55. Stephens WZ, Wiles TJ, Martinez ES, Jemielita M, Burns AR, Parthasarathy R, et al.
631 Identification of Population Bottlenecks and Colonization Factors during Assembly of
632 Bacterial Communities within the Zebrafish Intestine. *MBio* 2015; **6**: e01163-15.

633 56. Wright KJ, Seed PC, Hultgren SJ. Uropathogenic Escherichia coli flagella aid in
634 efficient urinary tract colonization. *Infect Immun* 2005; **73**: 7657–68.

635 57. Chiang P, Burrows LL. Biofilm formation by hyperpiliated mutants of Pseudomonas
636 aeruginosa. *J Bacteriol* 2003; **185**: 2374–8.

637 58. Déziel E, Comeau Y, Villemur R. Initiation of biofilm formation by Pseudomonas

aeruginosa 57RP correlates with emergence of hyperpiliated and highly adherent phenotypic variants deficient in swimming, swarming, and twitching motilities. *J Bacteriol* 2001.

59. Seminara A, Angelini TE, Wilking JN, Vlamakis H, Ebrahim S, Kolter R, et al. Osmotic spreading of Bacillus subtilis biofilms driven by an extracellular matrix. *Proc Natl Acad Sci* 2012.